Stable and Conservative High-Order Methods on Triangular Elements Using Tensor-Product Summation-by-Parts Operators

Tristan Montoya and David W. Zingg

Institute for Aerospace Studies, University of Toronto
4925 Dufferin St, Toronto, ON M3H 5T6, Canada

July 11, 2022

Introduction

Motivation for high-order methods

For smooth problems and low error tolerances, **high-order** and **spectral methods** are more accurate than second-order methods for a given number of degrees of freedom

Element-based high-order methods are particularly amenable to algorithms which are high in arithmetic intensity and therefore able to best exploit the floating-point performance of modern hardware

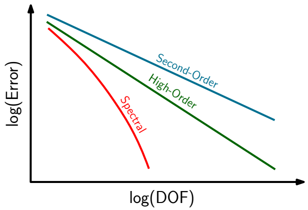

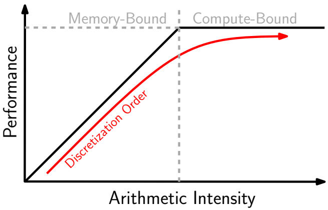

Introduction

Tensor-product vs. multidimensional approximations

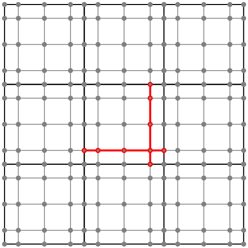

Tensor-product

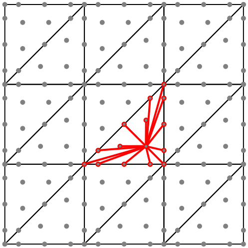

Multidimensional

- Fast evaluation of operators dimension by dimension (i.e. using **sum factorization**[1])
- Typically restricted to domains which map onto the square or cube

- Facilitates treatment of **complex geometries** and mesh adaptation
- Increased operation count at higher orders due to tighter coupling of DOFs

[1] Orszag, 1980

High-order methods in collapsed coordinates

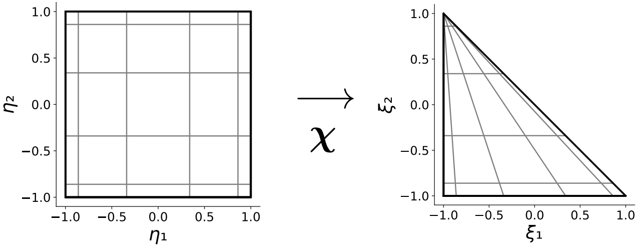

An alternative is to use a collapsed coordinate transformation to enable sum factorization on triangles or other element types[2]

Combines the efficiency of tensor-product approximations with the geometric flexibility of general multidimensional elements

[2]Approach proposed by Dubiner (1991); early applications to **continuous Galerkin** (CG) methods by Sherwin and Karniadakis (1995, 1996) and to **discontinuous Galerkin** (DG) schemes by Lomtev and Karniadakis (1999) and Kirby et al. (2000)

Introduction

High-order methods in collapsed coordinates

Collapsed-coordinate approach is now a fairly mature technology, forming the basis for triangular/tetrahedral/prismatic/pyramidal elements in ***Nektar++*** (Cantwell et al., 2015; Moxey et al., 2020)

Results in **efficient algorithms** on modern hardware, for example, with SIMD vectorization (Moxey, Amici, and Kirby, 2020)

However, high-order methods often **lack robustness** when used to solve nonlinear problems or with curvilinear meshes

Provably stable schemes offer a potential solution, as stability can be **guaranteed** *a priori* without relying on artificial dissipation, filtering, over-integration, or other *ad hoc* techniques

Introduction

Summation-by-parts property

The **summation-by-parts** (SBP) property provides a general framework for constructing and analyzing numerical methods in which provable properties are established at the discrete level by mimicking the corresponding continuous analysis

SBP approach has been used to construct provably stable high-order methods for linear and nonlinear problems on curvilinear meshes employing **quad/hex**[3] as well as **tri/tet**[4] elements

Can we exploit the computational benefits of collapsed coordinates alongside the provable stability afforded by the SBP property?

[3] Fisher and Carpenter, 2013; Gassner, 2013; Carpenter et al., 2014; Kopriva and Gassner, 2014; Gassner, Winters, and Kopriva, 2016.

[4] Hicken, Del Rey Fernández, and Zingg, 2016; Chen and Shu, 2017; Del Rey Fernández, Hicken, and Zingg, 2018; Crean et al., 2018; Chan, 2018.

Approximation in Collapsed Coordinates

One-dimensional nodal sets and basis functions

Define nodal sets $\{\eta_1^{(i)}\}_{i=0}^{q_1}$ and $\{\eta_2^{(i)}\}_{i=0}^{q_2}$ on $[-1, 1]$ such that

$$-1 \le \eta_1^{(0)} < \cdots < \eta_1^{(q_1)} \le 1, \quad -1 \le \eta_2^{(0)} < \cdots < \eta_2^{(q_2)} < 1,$$

associated with Lagrange polynomials $\{\ell_1^{(i)}\}_{i=0}^{q_1}$ and $\{\ell_2^{(i)}\}_{i=0}^{q_2}$ as well as positive quadrature weights $\{\omega_1^{(i)}\}_{i=0}^{q_1}$ and $\{\omega_2^{(i)}\}_{i=0}^{q_2}$

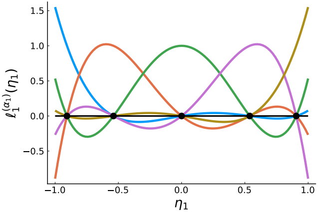

Legendre-Gauss (LG)

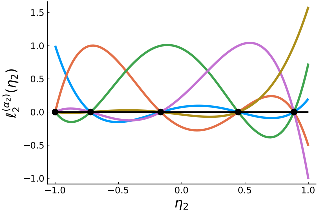

Legendre-Gauss-Radau (LGR)

Approximation in Collapsed Coordinates

Nodal tensor-product basis functions

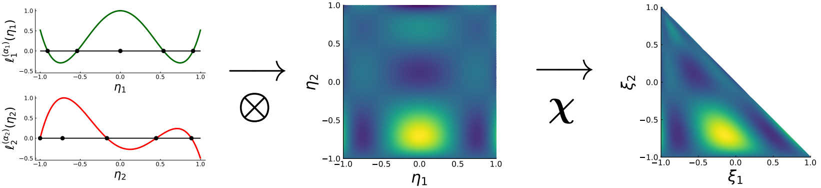

Nodal basis on $\hat{\mathcal{T}}^2 := \{\boldsymbol{\xi} \in [-1,1]^2 : \xi_1 + \xi_2 \leq 0\}$ given in terms of

$$\boldsymbol{\chi}(\boldsymbol{\eta}) := \begin{bmatrix} \frac{1}{2}(1+\eta_1)(1-\eta_2) - 1 \\ \eta_2 \end{bmatrix}$$

as

$$\ell^{(\sigma(\boldsymbol{\alpha}))}(\boldsymbol{\chi}(\boldsymbol{\eta})) := \ell_1^{(\alpha_1)}(\eta_1)\ell_2^{(\alpha_2)}(\eta_2),$$

ordered using $\sigma : \{0 : q_1\} \times \{0 : q_2\} \to \{1 : (q_1+1)(q_2+1)\}$

Approximation in Collapsed Coordinates

Volume and facet quadrature rules

Volume quadrature rule on $\hat{\mathcal{T}}^2$ has nodes and weights given by

$$\boldsymbol{\xi}^{(\sigma(\boldsymbol{\alpha}))} := \boldsymbol{\chi}\big(\eta_1^{(\alpha_1)}, \eta_2^{(\alpha_2)}\big), \quad \omega^{(\sigma(\boldsymbol{\alpha}))} := \frac{1-\eta_2^{(\alpha_2)}}{2}\omega_1^{(\alpha_1)}\omega_2^{(\alpha_2)}$$

On each edge $\hat{\mathcal{E}}^{(\zeta)} \subset \partial\hat{\mathcal{T}}^2$, define a **facet quadrature rule** with nodes $\{\boldsymbol{\xi}^{(\zeta,i)}\}_{i=1}^{N_\zeta}$ and non-negative weights $\{\omega^{(\zeta,i)}\}_{i=1}^{N_\zeta}$

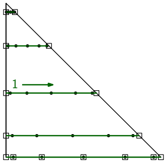

Facet quadrature nodes aligned

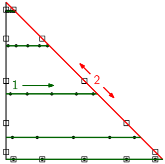

Facet quadrature nodes not aligned

Approximation in Collapsed Coordinates

Summation-by-parts operators on the reference element

Taking a spectral collocation approach, we can define the operators

$$
\begin{aligned}
D_{ij}^{(m)} &:= \frac{\partial \ell^{(j)}}{\partial \xi_m}(\boldsymbol{\xi}^{(i)}), \qquad & M_{ij} &:= \omega^{(i)}\delta_{ij}, \\
R_{ij}^{(\zeta)} &:= \ell^{(j)}(\boldsymbol{\xi}^{(\zeta,i)}), \qquad & B_{ij}^{(\zeta)} &:= \omega^{(\zeta,i)}\delta_{ij}
\end{aligned}
$$

Accuracy of $\underline{\underline{D}}^{(m)}$ and $\underline{\underline{R}}^{(\zeta)}$ follows from fact that the basis spans a space including all polynomials of up to degree $p = \min(q_1, q_2)$

Approximation in Collapsed Coordinates

Summation-by-parts operators on the reference element

For quadrature rules of at least degree $2q_1$ and $2q_2$ in the η_1 and η_2 directions,[5] $\underline{\underline{D}}^{(m)}$ is an SBP operator of degree p in the sense of Hicken, Del Rey Fernández, and Zingg (2016, Definition 2.1)

In particular, the **SBP property is satisfied** for $m \in \{1, 2\}$ as

$$\underline{\underline{M}}\,\underline{\underline{D}}^{(m)} + \big(\underline{\underline{D}}^{(m)}\big)^{\mathsf{T}} \underline{\underline{M}} = \sum_{\zeta=1}^{3} \hat{n}_m^{(\zeta)} \big(\underline{\underline{R}}^{(\zeta)}\big)^{\mathsf{T}} \underline{\underline{B}}^{(\zeta)} \underline{\underline{R}}^{(\zeta)},$$

mimicking the IBP relation on the reference element:

$$\int_{\hat{\mathcal{T}}^2} U \frac{\partial V}{\partial \xi_m} \, d\boldsymbol{\xi} + \int_{\hat{\mathcal{T}}^2} \frac{\partial U}{\partial \xi_m} V \, d\boldsymbol{\xi} = \sum_{\zeta=1}^{3} \int_{\hat{\mathcal{E}}^{(\zeta)}} UV \, \hat{n}_m^{(\zeta)} \, d\hat{s},$$

where $\hat{n}_m^{(\zeta)}$ is the m^{th} component of outward unit normal to $\hat{\mathcal{E}}^{(\zeta)}$

[5] See paper; one degree higher than for quad/hex (Kopriva and Gassner, 2010)

Curvilinear Meshes

Mapping from reference to physical coordinates

Consider a smooth, time-invariant mapping $\boldsymbol{X}^{(\kappa)} : \hat{\mathcal{T}}^2 \to \Omega^{(\kappa)}$, where $\Omega^{(\kappa)} \subset \mathbb{R}^2$ is an element in the mesh $\mathcal{T}^h := \{\Omega^{(\kappa)}\}_{\kappa=1}^{N_e}$

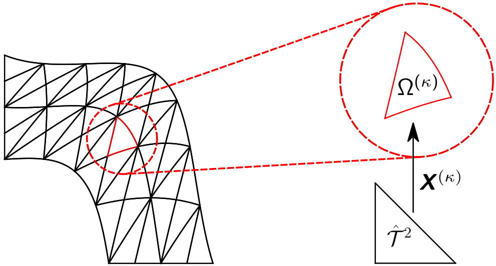

Define $J^{(\kappa)}(\boldsymbol{\xi}) := \det(\nabla_{\boldsymbol{\xi}} \boldsymbol{X}^{(\kappa)}(\boldsymbol{\xi}))$ where $\nabla_{\boldsymbol{\xi}} \boldsymbol{X}^{(\kappa)}(\boldsymbol{\xi}) \in \mathbb{R}^{2\times 2}$ is the Jacobian of the mapping, and assume $J^{(\kappa)}(\boldsymbol{\xi}) > 0$ for all $\boldsymbol{\xi} \in \hat{\mathcal{T}}^2$

Curvilinear Meshes

Summation-by-parts operators on mapped elements

Evaluate geometric terms at volume and facet quadrature nodes as

$$\begin{aligned}
J_{ij}^{(\kappa)} &:= J^{(\kappa)}(\boldsymbol{\xi}^{(i)})\delta_{ij}, \\
J_{ij}^{(\kappa,\zeta)} &:= \| J^{(\kappa)}(\boldsymbol{\xi}^{(\zeta,i)})(\nabla_{\xi}\boldsymbol{X}^{(\kappa)}(\boldsymbol{\xi}^{(\zeta,i)}))^{-\mathsf{T}}\hat{\boldsymbol{n}}^{(\zeta)}\|_2\delta_{ij}, \\
\Lambda_{ij}^{(\kappa,m,n)} &:= \left[J^{(\kappa)}(\boldsymbol{\xi}^{(i)})(\nabla_{\xi}\boldsymbol{X}^{(\kappa)}(\boldsymbol{\xi}^{(i)}))^{-1}\right]_{mn}\delta_{ij}, \\
N_{ij}^{(\kappa,\zeta,n)} &:= \left[J^{(\kappa)}(\boldsymbol{\xi}^{(\zeta,i)})(\nabla_{\xi}\boldsymbol{X}^{(\kappa)}(\boldsymbol{\xi}^{(\zeta,i)}))^{-\mathsf{T}}\hat{\boldsymbol{n}}^{(\zeta)}\right]_{n}\delta_{ij}
\end{aligned}$$

Skew-symmetric formulation from Crean et al. (2018) results in

$$\begin{aligned}
\underline{\underline{Q}}^{(\kappa,n)} := \frac{1}{2}\sum_{m=1}^{2}\left(\underline{\underline{\Lambda}}^{(\kappa,m,n)}\underline{\underline{M}}\,\underline{\underline{D}}^{(m)} - \left(\underline{\underline{D}}^{(m)}\right)^{\mathsf{T}}\underline{\underline{M}}\,\underline{\underline{\Lambda}}^{(\kappa,m,n)}\right) \\
+ \frac{1}{2}\sum_{\zeta=1}^{3}\left(\underline{\underline{R}}^{(\zeta)}\right)^{\mathsf{T}}\underline{\underline{B}}^{(\zeta)}\underline{\underline{N}}^{(\kappa,\zeta,n)}\underline{\underline{R}}^{(\zeta)}
\end{aligned}$$

Curvilinear Meshes

Summation-by-parts operators on mapped elements

Derivative operator $\underline{\underline{D}}^{(\kappa,\zeta)} := (\underline{\underline{M}}\,\underline{\underline{J}}^{(\kappa)})^{-1}\underline{\underline{Q}}^{(\kappa,\zeta)}$ is an approximation of order $p = \min(q_1, q_2)$ to $\partial/\partial x_n$ (Crean et al., 2018, Theorem 5), and satisfies the SBP property on the **physical element** as

$$\underline{\underline{Q}}^{(\kappa,n)} + \left(\underline{\underline{Q}}^{(\kappa,n)}\right)^{\mathsf{T}} = \sum_{\zeta=1}^{3} \left(\underline{\underline{R}}^{(\zeta)}\right)^{\mathsf{T}} \underline{\underline{B}}^{(\zeta)} \underline{\underline{N}}^{(\kappa,\zeta,n)} \underline{\underline{R}}^{(\zeta)}$$

A **conservative**, **free-stream-preserving**, and **energy stable** discretization of order p, approximating the weak DG formulation

$$\int_{\Omega^{(\kappa)}} \left(V\partial_t U - \nabla_{\boldsymbol{x}} V \cdot \boldsymbol{F}\right) d\Omega + \int_{\partial\Omega^{(\kappa)}} VF^*\, d\Gamma = 0,$$

is then given by

$$\underline{\underline{M}}\,\underline{\underline{J}}^{(\kappa)} \frac{d\underline{u}^{(h,\kappa)}}{dt} = \overbrace{\sum_{n=1}^{2} \left(\underline{\underline{Q}}^{(\kappa,n)}\right)^{\mathsf{T}} \underline{f}^{(h,\kappa,n)} - \sum_{\zeta=1}^{3} \left(\underline{\underline{R}}^{(\zeta)}\right)^{\mathsf{T}} \underline{\underline{B}}^{(\zeta)} \underline{f}^{(*,\kappa,\zeta)}}^{=:\,\underline{r}^{(h,\kappa)}}$$

Curvilinear Meshes

Comparison of operator evaluation strategies for $\underline{\underline{Q}}^{(\kappa,n)}$

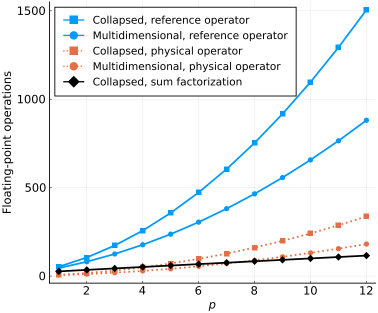

Operations per DOF

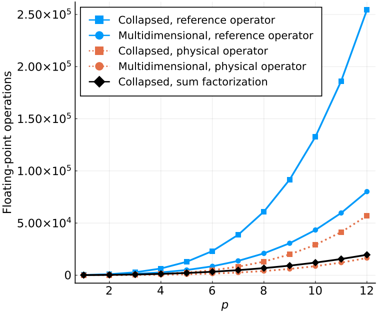

Total floating-point operations

Collapsed: Proposed tensor-product operators in collapsed coordinates using $(p+1)^2$ volume quadrature nodes and $p+1$ facet quadrature nodes per edge (volume and facet quadrature nodes aligned but not collocated)

Multidimensional: Nodal SBP scheme with $(p+1)(p+2)/2$ volume quadrature nodes, $p+1$ non-collocated facet quadrature nodes per edge

Modal Formulation

Motivation

Tensor-product nodal basis in collapsed coordinates allows for fast matrix-free operator evaluation, but suffers from two drawbacks:

- Maximum stable time step (i.e. CFL limit) is restricted due to "clustering" of resolution at the singularity (Dubiner, 1991)
- Representing solution directly in the nodal basis requires $(p+1)^2$ DOF per element for a scheme of degree p, which is larger than the dimension of the total-degree polynomial space, which does not support a tensor-product nodal basis

Modal Formulation

Basis functions

Dubiner (1991) suggests to use a modal basis[6] of the form

$$\phi^{(\pi(\boldsymbol{\alpha}))}(\boldsymbol{\chi}(\boldsymbol{\eta})) := \underbrace{\sqrt{2}P_{\alpha_1}^{(0,0)}(\eta_1)}_{=:\,\psi_1^{(\alpha_1)}(\eta_1)}\underbrace{(1-\eta_2)^{\alpha_1}P_{\alpha_2}^{(2\alpha_1+1,0)}(\eta_2)}_{=:\,\psi_2^{(\alpha_1,\alpha_2)}(\eta_2)},$$

ordered as $\pi : \{\boldsymbol{\alpha} \in \mathbb{N}_0^2 : \alpha_1 + \alpha_2 \leq p\} \to \{1 : (p+1)(p+2)/2\}$

The PKD basis is characterized by the following properties:

- **Orthogonal** with respect to standard L^2 inner product on $\hat{\mathcal{T}}^2$
- “Warped” tensor-product of polynomials in collapsed coordinates – **amenable to sum factorization algorithms**

[6] Introduced by Proriol (1957); see also Koornwinder (1975)

Modal Formulation

Residual evaluation

Generalized Vandermonde matrix with entries $V_{ij} = \phi^{(j)}(\boldsymbol{\xi}^{(i)})$ or its transpose can be applied in $O(p^3)$ operations for $q_1 = q_2 = p$

To obtain the semi-discrete residual for the modal approach:

1. Apply $\underline{\underline{V}}$ to modal expansion coefficients $\underline{\tilde{u}}^{(h,\kappa)}$ in order to obtain nodal values $\underline{u}^{(h,\kappa)}$
2. Evaluate nodal fluxes, apply nodal operators to obtain $\underline{r}^{(h,\kappa)}$
3. Apply $\underline{\underline{V}}^{\mathsf{T}}$ and invert[7] $\underline{\underline{V}}^{\mathsf{T}}\underline{\underline{M}}\,\underline{\underline{J}}^{(\kappa)}\underline{\underline{V}}$ to obtain $d\underline{\tilde{u}}^{(h,\kappa)}/dt$

Modal approach retains provable **stability**, **conservation**, and **free-stream preservation** properties of nodal formulation

[7] Local mass matrix is dense for curved elements, but tensor-product structure and positive-definiteness make it amenable to iterative methods such as PCG (Pazner and Persson, 2018); entire residual is $O(p^3)$ if number of iterations is independent of p.

Numerical Experiments

Problem setup and mesh

Solve the **linear advection equation** with a constant wave speed of $\boldsymbol{a} := [1, 1]^{\mathsf{T}}$ on a periodic square domain $\Omega := (0, 1)^2$

Warp a uniform mesh with N_e elements using Lagrange basis of degree p to mimic high-order meshing of complex geometries

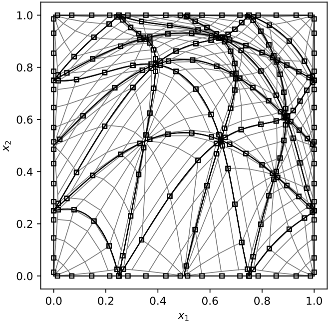

Example mesh for $p = 4$ and $N_e = 32$

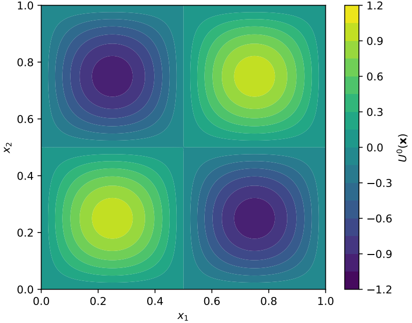

Sinusoidal initial condition

Numerical Experiments

Semi-discrete operator spectra for $p = 4$ and $N_e = 32$

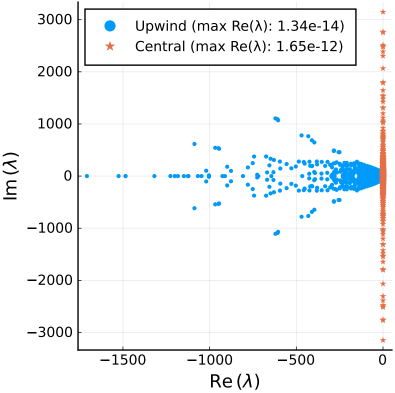

Nodal formulation

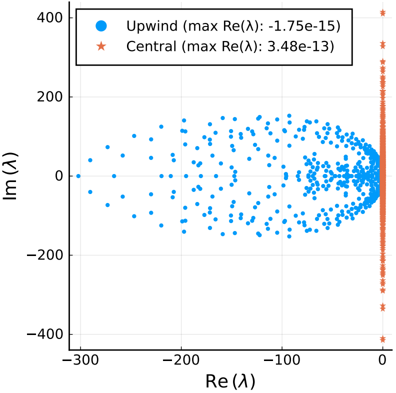

Modal formulation

Numerical Experiments

Grid refinement studies (reference 5th and 10th order slopes pictured)

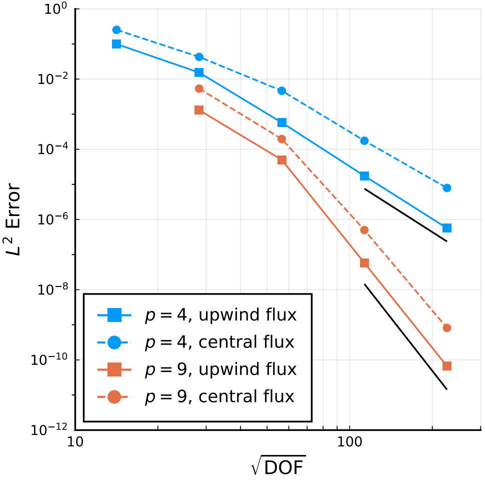

Nodal formulation

- ✓ Conservative
- ✓ Energy dissipative for upwind flux
- ✓ Energy conservative for central flux

Numerical Experiments

Grid refinement studies (reference 5^{th} and 10^{th} order slopes pictured)

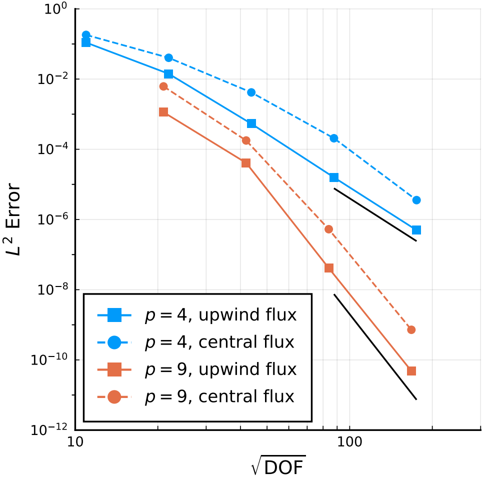

Modal formulation

- ✓ Conservative
- ✓ Energy dissipative for upwind flux
- ✓ Energy conservative for central flux

Numerical Experiments

Grid refinement studies (reference 5th and 10th order slopes pictured)

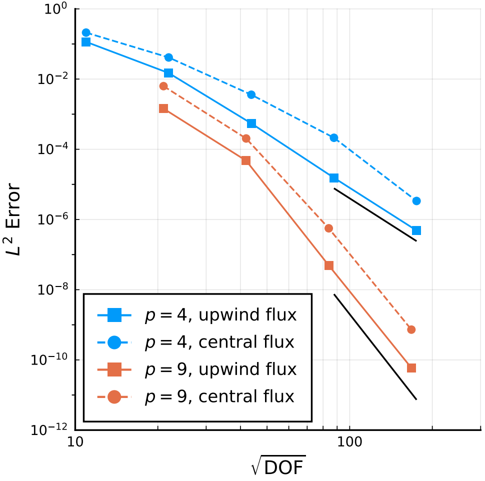

Standard weak-form DG method

- ✓ Conservative
- ✓ Energy dissipative for upwind flux
- ✗ Energy conservative for central flux

Conclusions

By **extending the SBP approach to tensor-product discretizations in collapsed coordinates**, we have laid the theoretical groundwork for robust schemes suitable for complex geometries which extend efficiently to arbitrary order

Presented **nodal formulation** (diagonal mass matrix in curvilinear coordinates, solution directly available at quadrature nodes) and **modal formulation** (minimal DOF, allows for larger time steps)

Future work includes three-dimensional problems, entropy-stable discretizations of nonlinear conservation laws, alternative nodal approaches with reduced spectral radii, and efficiency comparisons

https://www.researchgate.net/profile/Tristan-Montoya · https://github.com/tristanmontoya

References I

Cantwell, C. D. et al. (July 2015). "Nektar++: An open-source spectral/hp element framework." *Computer Physics Communications* 192, pp. 205–219.

Carpenter, M. H. et al. (Oct. 2014). "Entropy Stable Spectral Collocation Schemes for the Navier-Stokes Equations: Discontinuous Interfaces." *SIAM Journal on Scientific Computing* 36.5, B835–B867.

Chan, J. (June 2018). "On Discretely Entropy Conservative and Entropy Stable Discontinuous Galerkin Methods." *Journal of Computational Physics* 362, pp. 346–374.

Chen, T. and C.-W. Shu (Sept. 2017). "Entropy Stable High Order Discontinuous Galerkin Methods with Suitable Quadrature Rules for Hyperbolic Conservation Laws." *Journal of Computational Physics* 345, pp. 427–461.

References II

Crean, J. et al. (Mar. 2018). "Entropy-Stable Summation-by-Parts Discretization of the Euler Equations on General Curved Elements." *Journal of Computational Physics* 356, pp. 410–438.

Del Rey Fernández, D. C., J. E. Hicken, and D. W. Zingg (Apr. 2018). "Simultaneous Approximation Terms for Multi-dimensional Summation-by-Parts Operators." *Journal of Scientific Computing* 75.1, pp. 83–110.

Dubiner, M. (Dec. 1991). "Spectral Methods on Triangles and Other Domains." *Journal of Scientific Computing* 6.4, pp. 345–390.

Fisher, T. C. and M. H. Carpenter (Nov. 2013). "High-order Entropy Stable Finite Difference Schemes for Nonlinear Conservation Laws: Finite domains." *Journal of Computational Physics* 252, pp. 518–557.

References III

Gassner, G. J. (May 2013). "A Skew-Symmetric Discontinuous Galerkin Spectral Element Discretization and Its Relation to SBP-SAT Finite Difference Methods." *SIAM Journal on Scientific Computing* 35.3, A1233–A1253.

Gassner, G. J., A. R. Winters, and D. A. Kopriva (Dec. 2016). "Split Form Nodal Discontinuous Galerkin Schemes with Summation-by-Parts Property for the Compressible Euler Equations." *Journal of Computational Physics* 327, pp. 39–66.

Hicken, J. E., D. C. Del Rey Fernández, and D. W. Zingg (July 2016). "Multidimensional Summation-by-Parts Operators: General Theory and Application to Simplex Elements." *SIAM Journal on Scientific Computing* 38.4, A1935–A1958.

Kirby, R. M. et al. (May 2000). "A Discontinuous Galerkin Spectral/*hp* Method on Hybrid grids." *Applied Numerical Mathematics* 33.1-4, pp. 393–405.

References IV

- Koornwinder, T. (1975). "Two-Variable Analogues of the Classical Orthogonal Polynomials." *Theory and Application of Special Functions*. Ed. by R. Askey. Elsevier, pp. 435–495.
- Kopriva, D. A. and G. J. Gassner (Aug. 2010). "On the Quadrature and Weak Form Choices in Collocation Type Discontinuous Galerkin Spectral Element Methods." *Journal of Scientific Computing* 44, pp. 136–155.
- — (Aug. 2014). "An Energy Stable Discontinuous Galerkin Spectral Element Discretization for Variable Coefficient Advection Problems." *SIAM Journal on Scientific Computing* 36.4, A2076–A2099.
- Lomtev, I. and G. E. Karniadakis (Mar. 1999). "A discontinuous Galerkin method for the Navier–Stokes equations." *International Journal for Numerical Methods in Fluids* 29.5, pp. 587–603.

References V

Moxey, D., R. Amici, and R. M. Kirby (May 2020). “Efficient Matrix-Free High-Order Finite Element Evaluation for Simplicial Elements.” *SIAM Journal on Scientific Computing* 42.3, pp. C97–C123.

Moxey, D. et al. (Apr. 2020). “Nektar++: Enhancing the capability and application of high-fidelity spectral/hp element methods.” *Computer Physics Communications* 249, p. 107110.

Orszag, S. A. (Aug. 1980). “Spectral Methods for Problems in Complex Geometries.” *Journal of Computational Physics* 37.1, pp. 70–92.

Pazner, W. and P.-O. Persson (Feb. 2018). “Approximate Tensor-Product Preconditioners for Very High Order Discontinuous Galerkin Methods.” *Journal of Computational Physics* 354, pp. 344–369.

References VI

Proriol, J. (Dec. 1957). "Sur Une Famille De Polynomes à Deux Variables Orthogonaux Dans Un Triangle." *Comptes Rendus Hebdomadaires des Séances de l'Académie des Sciences* 245, pp. 2459–2461.

Sherwin, S. J. and G. E. Karniadakis (June 1995). "A Triangular Spectral Element Method: Applications to the Incompressible Navier-Stokes Equations." *Computer Methods in Applied Mechanics and Engineering* 123.1-4, pp. 189–229.

Sherwin, S. J. and G. E. Karniadakis (Mar. 1996). "Tetrahedral *hp* Finite Elements: Algorithms and Flow Simulations." *Journal of Computational Physics* 124.1, pp. 14–45.